15B.5 OPERATIONAL 2-H THUNDERSTORM GUIDANCE FORECASTS TO 24 HOURS ON A 20-KM GRID

Jerome P. Charba*
Frederick G. Samplatsky
Meteorological Development Laboratory
Office of Science and Technology
National Weather Service
Silver Spring, Maryland

1. INTRODUCTION

Weather related air traffic congestion is a major problem for the air transportation industry. Thunderstorms, especially in the vicinity of airports, comprise one of several weather types that account for the vast majority of the aviation disruptions. The National Weather Service (NWS) provides air traffic managers with convective forecast products for tactical and strategical aviation operations. A key product for tactical operations near airports is the Collaborative Convective Forecast Product (CCFP, http://weather.gov/infoservicechanges/CCFP_PDD_Enhancement.pdf), whereby the Aviation Weather Center of the NWS National Centers for Environmental Prediction (NCEP) provides convective weather guidance to 6 hours 11 times per day for the contiguous U.S. (CONUS) during the convective season. Another important product for strategical flight planning is the Terminal Aerodrome Forecast (TAF) (NWS 2008), which is produced every 6 hours by NWS Weather Forecast Offices for airports over the U.S. TAFs contain information on expected aviation-sensitive weather, including thunderstorms, up to 30 hours in advance.

Also, cloud-to-ground (CTG) lightning results in a long term annual average of 62 fatalities over the U.S. (http://www.weather.gov/os/hazstats.shtml), which is more than that resulting from tornadoes. Thus, thunderstorms pose a serious safety threat to the public.

The Meteorological Development Laboratory is addressing the need for improved convective weather information in aviation and public forecasts by providing statistically-based gridded thunderstorm forecast guidance products. One of the present operational products consists of probability and categorical occurrence/non-occurrence forecasts of one or more cloud-to-ground (CTG) lightning strikes in 20-km grid boxes for 2-h periods out to 24 hours (Charba and Liang 2005a, henceforth cited as CL). This guidance product is issued at hourly intervals (24 times daily) throughout the year. This article describes properties of the grid-oriented statistical model, a significant geographical regionalization problem that required treatment, forecast performance scores, and operational aspects.

2. GEOGRAPHICAL REGIONALIZATION: TREATING BOUNDARY DISCONTINUITIES

A grid-oriented LAMP (Localized Aviation MOS Program) approach (Ghirardelli and Glahn 2009) is used to produce the thunderstorm occurrence probabilities. This method uses multiple linear regression equations to produce probability forecasts at grid points rather than at stations; the latter approach applies to all other aviation weather elements in the LAMP product suite. The predictors in the thunderstorm probability equations are based on current CTG lightning reports (Cummins et al. 1998), current quality controlled radar reflectivity measurements (Charba and Liang 2005b), MOS thunderstorm probability forecasts from the latest 6-hourly cycle (Hughes 2004), and fine scale lightning climatology and topography. A wide range of predictors are derived from these data inputs on a 20-km grid that spans the CONUS (see CL for details).

An important feature of the thunderstorm probability regression equations is their geographical stratification, whereby a separate regression equation applies to each region (Lowry and Glahn 1976). [Charba and Samplatsky (2009a) demonstrated the benefits of a regionalized approach over a corresponding non-regionalized analog with a similar statistical model for producing quantitative precipitation forecasts.] Initially, the 13 regions used were “discrete” areas, which were formed by

* *Corresponding author address:*
Dr. Jerome P. Charba, National Weather Service
1325 East West Highway, Room 10410
Silver Spring, MD 20910-3283
email: jerome.charba@noaa.gov

a simple partitioning of the CONUS domain (Fig. 1).

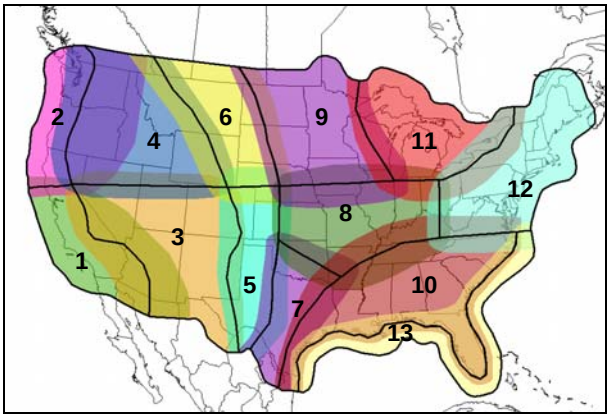

Figure 1. Discrete regions, which are bounded by bold black lines and numbered 1 to 13, and corresponding overlapping regions (color shading) for the spring season. The color shades change where neighboring regions overlap.

However, a problem arose with the discrete regions regression equations, as objectionable non-meteorological discontinuities appeared along region boundaries, even with the application of grid smoothing. An example probability field (Fig. 2a), which is for the 7-9 h projection from 0900 UTC 18 March 2008, illustrates the problem. Note that an artificial discontinuity, which extends from South Texas to northeast Arkansas, lies along the discrete region boundary that separates regions 7 and 8 from region 10 (Fig. 1). It stems from independent derivation of the equations among the regions, which results in regional variations in the thunderstorm predictor variables and regression coefficients. The latter are due to geographical variations in thunderstorm forcing mechanisms, predictability, and climatology. In fact, regional variations in the thunderstorm climatology alone can cause the discontinuities.

It is noted that inter-regional forecast inconsistency is a common property of regionalized statistical models. However, the problem may escape notice with the usual station-oriented approach because the randomly spaced station forecasts are not usually mapped. Also, in the early gridded model applications (see references in Charba and Samplatsky 2009a), the grids were relatively coarse and conventional grid smoothing could be used to control artificial spatial irregularities at region boundaries. Experience has shown that as the grid mesh comes down to around 20 km such smoothing is no longer effective. Clearly, treatment of the problem is warranted, as discontinuities such as those in Fig. 2a would undermine user acceptance of the guidance.

The discontinuity problem was addressed through two modifications of the developmental procedure. One modification consisted of expanding the discrete regions, which results in overlap of neighboring regions. The overlapping regions used for the spring season (March 16 – June 30) regression equations are shown in Fig. 1. The overlapping regions were smaller for the summer season (July 1 – October 15) and larger for the cool season (October 16 – March 15; not shown).

Overlap among neighboring regions results in a measure of consistency in regression equations based on them, as portions of the developmental samples are shared. However, the overlapping-regions equations were applied only to grid points within the original discrete regions (overlap portions of the regions were not used), as a sound procedure for dealing with multiple probabilities in region overlap zones was not available. Figure 2b shows the probability field resulting from this overlapping regions approach. Note that while the intensity of the regional discontinuities is diminished, the probability pattern was still judged unacceptable.

Thus, a second procedure, consisting of conditional smoothing along the region boundaries, was developed for treating the residual discontinuities. Specifically, where the probability gradient for a point on the boundary exceeds a pre-determined threshold, the probabilities in the immediate neighborhood are smoothed. The prescribed probability gradient threshold varied as a function of the forecast projection and the probability value. The localized smoothing along the boundaries was applied recursively until all boundary points passed the gradient check or an upper limit on the number of passes was reached.

The probability gradient thresholds and smoothing weights were “tuned” on the basis of extensive testing. The aim was to apply the least smoothing that yields acceptable probability patterns. The tuned smoothing was configured to be small (large) for the short (long) forecast projections and the low (high) probability values.

The probability field based on the overlapping regions regression equations and conditional boundary smoothing is shown in Fig. 2c. Note that

while slight evidence of the discontinuities in Fig. 2b remains, the probability pattern was judged acceptable. This finding was true based on tests with a large number of cases, which spanned all forecast projections and all three seasons.

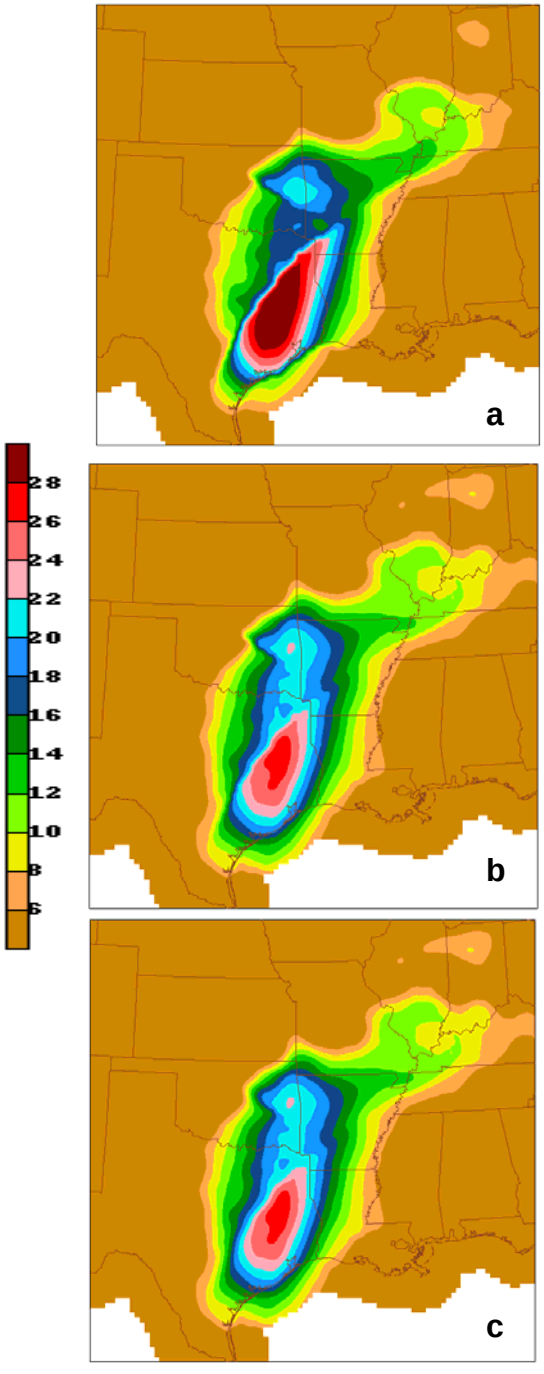

Figure 2. Thunderstorm probability (%) for the 7-9 h projection from 0900 UTC 18 March 2008 with (a) discrete regions, (b) overlapping regions, and (c) overlapping regions along with boundary smoothing.

Skill scores were computed to see what impact the discontinuity treatment may have had on forecast performance. The skill measure was the Brier score (Brier 1950) improvement on climatology (Brier skill score), where the predictand relative frequency computed at each grid point and time of the day from 15 years of historical data was used as a climatology surrogate. Figure 3 shows the Brier skill score for the 0900 UTC LAMP cycle, three selected forecast projections (henceforth the forecast projections refer to the ending times of the 2-h valid periods), two cool season (16 October 2006 – 15 March 2007 and 16 October 2007 – 15 March 2008) and two summer season (1 July – 15 October, 2007-2008) independent samples. The figure shows that the discontinuity treatment had a negligible impact on the scores.

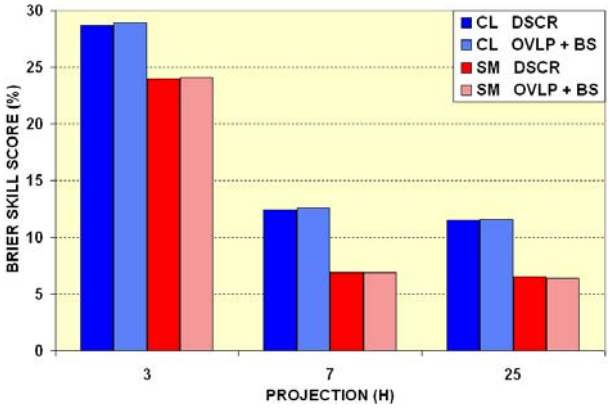

Figure 3. Brier skill score for the 0900 UTC thunderstorm probabilities at the projections (applicable to the ending times of the 2-h valid periods) indicated during the cool season (CL) and summer (SM) seasons. Additional notations in the legend are: DSCR = discrete regions; OVLP + BS = overlap regions and (region) boundary smoothing.

[It is noted that an improved method for treating the discontinuity problem was developed during late phases of implementation of the LAMP thunderstorm program. The new method, which was developed for fine grid quantitative precipitation prediction with a similar regionalized statistical model (Charba and Samplatsky 2009b), retains the regions overlap approach for deriving the regression equations, but the equations are applied to the overlapping regions rather than the discrete regions. Then, an objective weighting technique is used for blending multiple forecasts for grid points in the overlap zones. This method removes all traces of the discontinuities, and thus it is much preferred to the boundary smoothing technique described above. However, its incorporation into

the LAMP thunderstorm program was not undertaken, as the required re-development of previously completed LAMP cycles was not justified.]

3. FORECAST PERFORMANCE SCORES

The performance of archived real time 2-h thunderstorm probability and categorical forecasts was objectively scored for recent full season samples. The performance of the probabilities was measured with the Brier skill score, as defined previously, whereas performance of the categorical occurrence/non-occurrence forecasts was measured with the threat score [same as the critical success index, Schaefer (1990)], where relatively high (low) values indicate high (low) forecast accuracy.

For the 0900 UTC LAMP cycle and the entire CONUS domain, Figs. 4a and 4b show the Brier skill and threat scores, respectively, over a full "cool season" (16 October 2007 – 15 March 2008) and a full "summer season" (1 July 2007 – 15 October 2007) sample. The 0900 UTC cycle was chosen among the 24 cycles to examine LAMP thunderstorm forecast performance, as it was one of four cycles in which the latest hourly observational data provides the greatest updating contribution to the ingested 6-hourly MOS thunderstorm probability forecasts.

A major feature in both charts in Fig. 4 is that the scores are generally better during the cool season than during the summer. This result likely reflects the predominance of synoptic scale forcing of thunderstorms during the cool season, which is well predicted by operational numerical prediction models, versus mostly mesoscale forcing during the summer. Another major feature is the sharp maximum in forecast performance at the initial (3-h) projection and the rapid fall in performance thereafter. This feature reflects the strong predictive value of the most recent lightning strike and radar reflectivity measurements, which rapidly decreases over subsequent projections.

An interesting feature in Fig. 4 is the slight minimum in forecast performance at the 7 - 9 h projection. This performance minimum, which is characteristic of the early morning (0300 – 1200 UTC) cycles, may be due to the transitions from the convective maximum during the late night hours to the convective minimum during mid-morning and to subsequent convective maxima during the afternoon or (subsequent) night time hours. For the summer, a prominent secondary peak in the threat score occurs during the afternoon (around the 13-h projection in Fig. 4b), whereas for the cool season, a very weak secondary peak in Brier skill appears several hours later (around the 17-h projection). The correspondence of relatively high forecasting skill and the diurnal peaks in convective activity appears to be an inherent property of the LAMP forecast performance, as this feature was noted in all cycles. [It is worth noting that the corresponding 0900 UTC forecast performance profiles for the spring season (not shown) lie roughly between those for the summer and cool seasons (Fig. 4).]

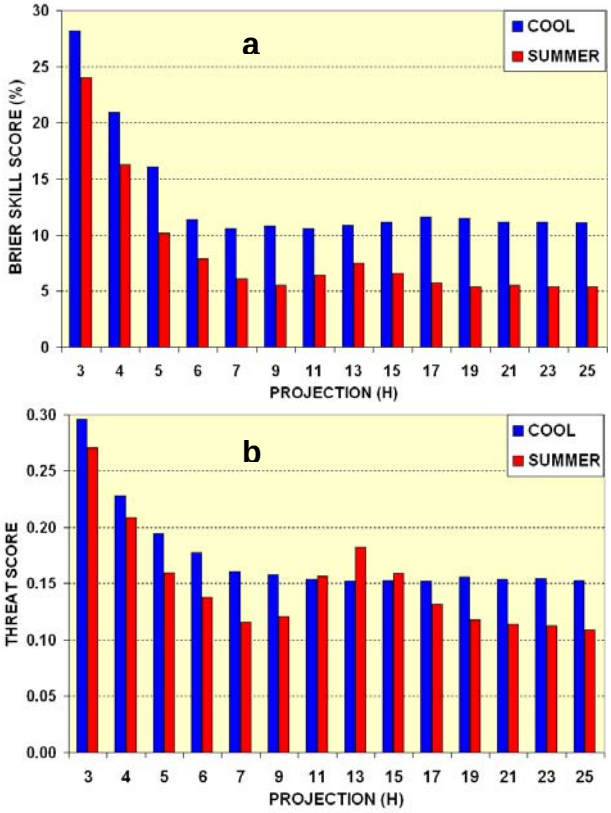

Figure 4. (a) Brier skill score for 2-h thunderstorm probabilities and (b) threat score for corresponding occurrence/non-occurrence forecasts as a function of projection for the 0900 UTC cycle. "Cool" ("summer") indicates cool (summer) season regression equations; the forecast projections apply to the ending times of the 2-h valid periods. Note that the forecast projections are at one-hour increments (and thus the valid periods overlap) to seven hours, and they are at 2-h increments thereafter.

4. CASE EXAMINATIONS

In this section, the thunderstorm probability forecasts are examined for two cases to discuss properties that may have practical value to users. Figure 5 is a case of a thunderstorm outbreak over the eastern U.S. on 8 - 9 June 2008, where the probabilities at the forecast projections indicated comprise the left and center columns of the image panel and the right column is the observed number of CTG lightning strikes during the corresponding valid periods. For example, Fig. 5a shows the 6-h probability from the 1500 UTC cycle (left frame), the 3-h probability from the 1800 UTC cycle (center frame), and the observed number of CTG lightning strikes for both forecasts for the 2-h period ending at 2100 UTC 8 June 2008 (right frame). Figures 5b and 5c have similar conventions for other projections and cycles for this case.

Several findings from Fig. 5 are noteworthy. One is that the probability patterns at the 6- and 9-h forecast projections (left column of panel) exhibit weaker areal focus and much lower peak values than those for the 3-h projections (center

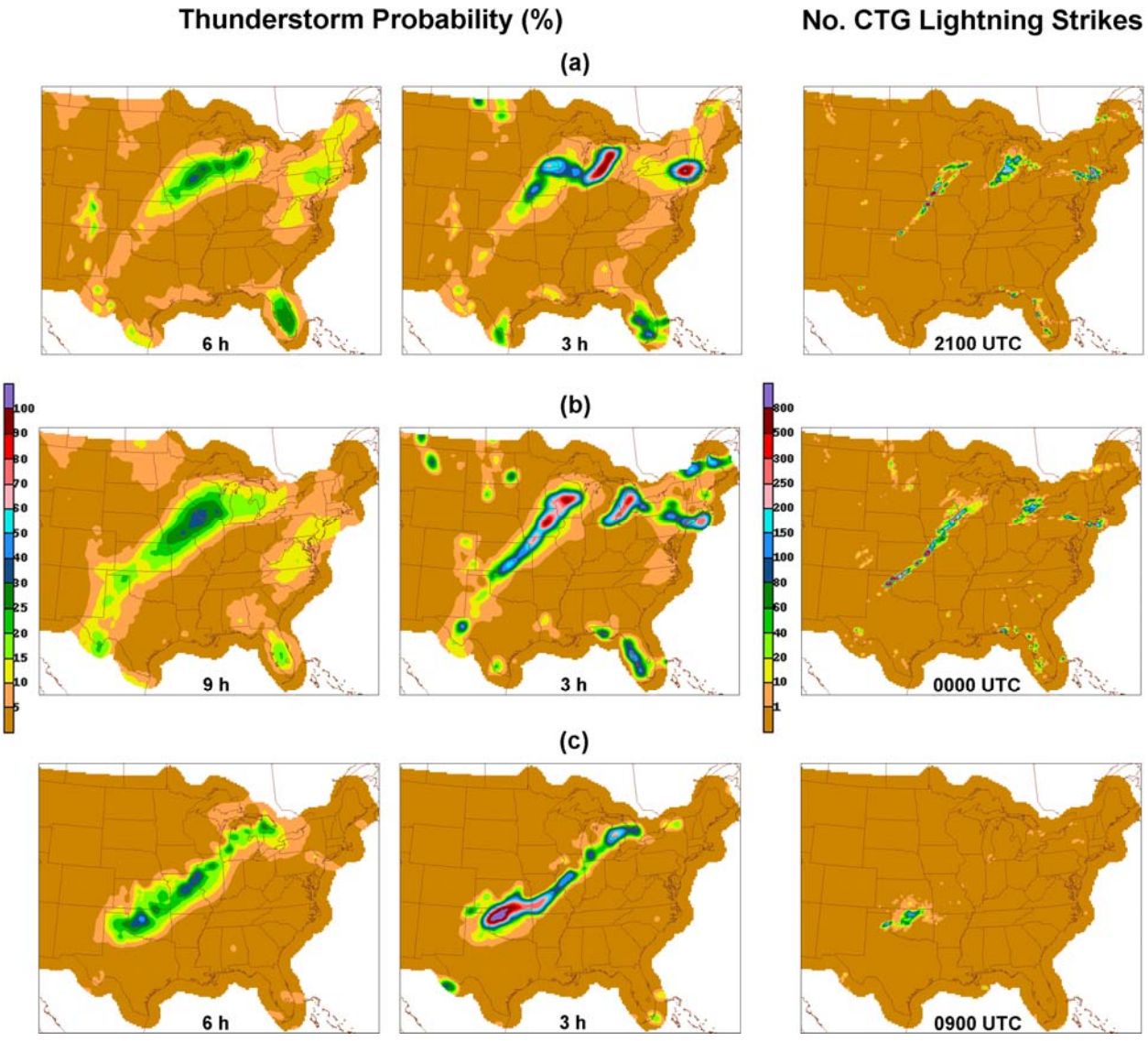

Figure 5. Two-hour thunderstorm probability (left and center columns) at the indicated forecast projection, and the observed number of CTG lightning strikes (right column) for the indicated valid time. The date for (a) is 8 June 2008, whereas (b) and (c) are for 9 June 2008. The forecast projection, valid time, and date each refers to the end of the 2-h valid period.

column of panel). This contrast in probability patterns between the 6 - 9 h projections and the initial projection becomes even greater as the longer projections are extended to the upper end of the projection range (not shown). Another feature in Fig. 5 is that the probabilities at the 3-h projections match the verifying lightning fields much better than the probabilities at the 6 – 9 h projections. In fact, the 3-h probability patterns accurately match the observed fields even for the fine details, especially during the growth phase of the convective event [Figs. 5a and 5b; for the 3-h projection during the decay phase (Fig, 5c), the probabilities appear excessive from Missouri to Michigan in this case]. These findings exemplify the LAMP concept, whereby the latest observational (lightning and radar) data is used to furnish detailed updates to longer range forecasts from earlier cycles.

As a contrasting (tropical) case, Figure 6a shows a 3-h thunderstorm probability forecast from 1200 UTC 1 September 2008, during which time the eye of Hurricane Gustav was making landfall at point "X" on the Louisiana coast. Figure 6b shows the number of CTG lightning strikes during this time, and Fig. 6c shows the radar estimated precipitation for the 6-h period ending 1800 UTC 1 September 2008. Note that thunderstorm probabilities are below 10 % for the location of the storm center, while peak probabilities of only 30–40 % appear along the northeast perimeter of the heavy precipitation area. These low probabilities match well the dearth of CTG lightning near the storm center and the low lightning counts even in the fringe areas of the storm. This combination of low LAMP thunderstorm probabilities and low levels of CTG lightning, despite the coincidence of heavy rainfall, is a common finding for tropical storm cases.

5. OPERATIONAL ASPECTS AND PRODUCT USAGE

The operational LAMP thunderstorm system consists of 24 hourly cycles (year round), which were recently phased in at NCEP Central Operations. The first cycle, which was for 0900 UTC, was implemented in July 2006, and the final four cycles were implemented in November 2008. The forecasts extend to 24 hours at even-hour cycle

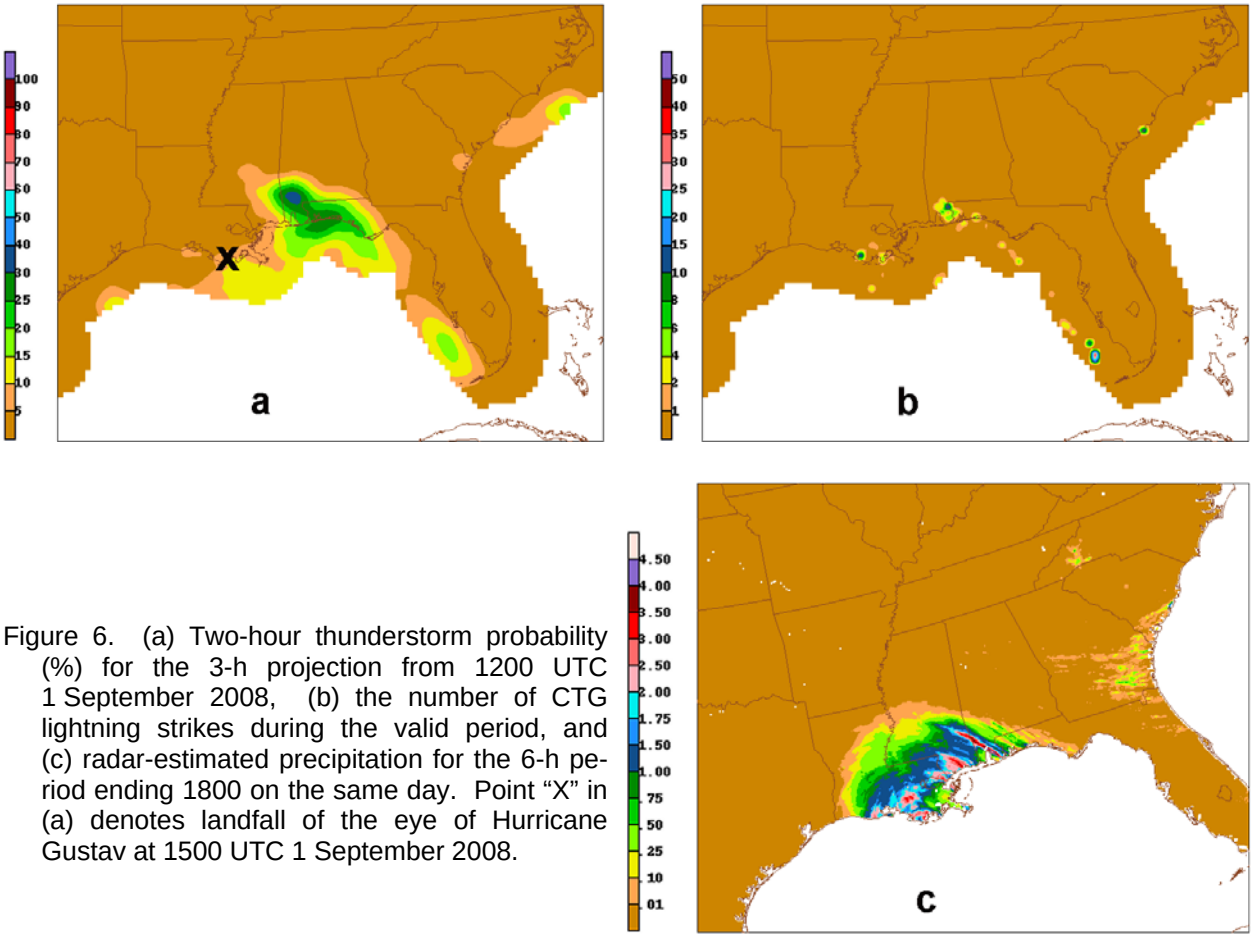

Figure 6. (a) Two-hour thunderstorm probability (%) for the 3-h projection from 1200 UTC 1 September 2008, (b) the number of CTG lightning strikes during the valid period, and (c) radar-estimated precipitation for the 6-h period ending 1800 on the same day. Point "X" in (a) denotes landfall of the eye of Hurricane Gustav at 1500 UTC 1 September 2008.

times and 25 hours for odd-hour cycle times. The probability and categorical forecasts are available to the entire weather enterprise through the NWS communication networks and the World Wide Web (http://weather.gov/mdl/gfslamp/ tstorm.php).

As indicated in the Introduction, the LAMP thunderstorm probability and categorical products were designed largely for use as guidance to the aviation weather prediction community. Also, efforts are ongoing to aid aviation weather forecasters in maximizing the guidance utility of the products. For example, a contractor for the Federal Aviation Administration (FAA) has recently conducted a preliminary comparative performance evaluation of the thunderstorm probabilities with the CCFP product (private communication). Also, another FAA contractor has created a "hybrid product", whereby the LAMP thunderstorm probabilities are overlaid on the corresponding CCFP graphic (Fig. 7). The operational utility of this chart for flight planning is presently being assessed. Further, MDL is coordinating with the FAA and others to assist users of the LAMP aviation weather guidance (including the thunderstorm probability and categorical products) in weather event decision making (see Ghirardelli and Glahn 2009). The overall objective of these efforts is to maximize the utility of the various guidance products in practical applications.

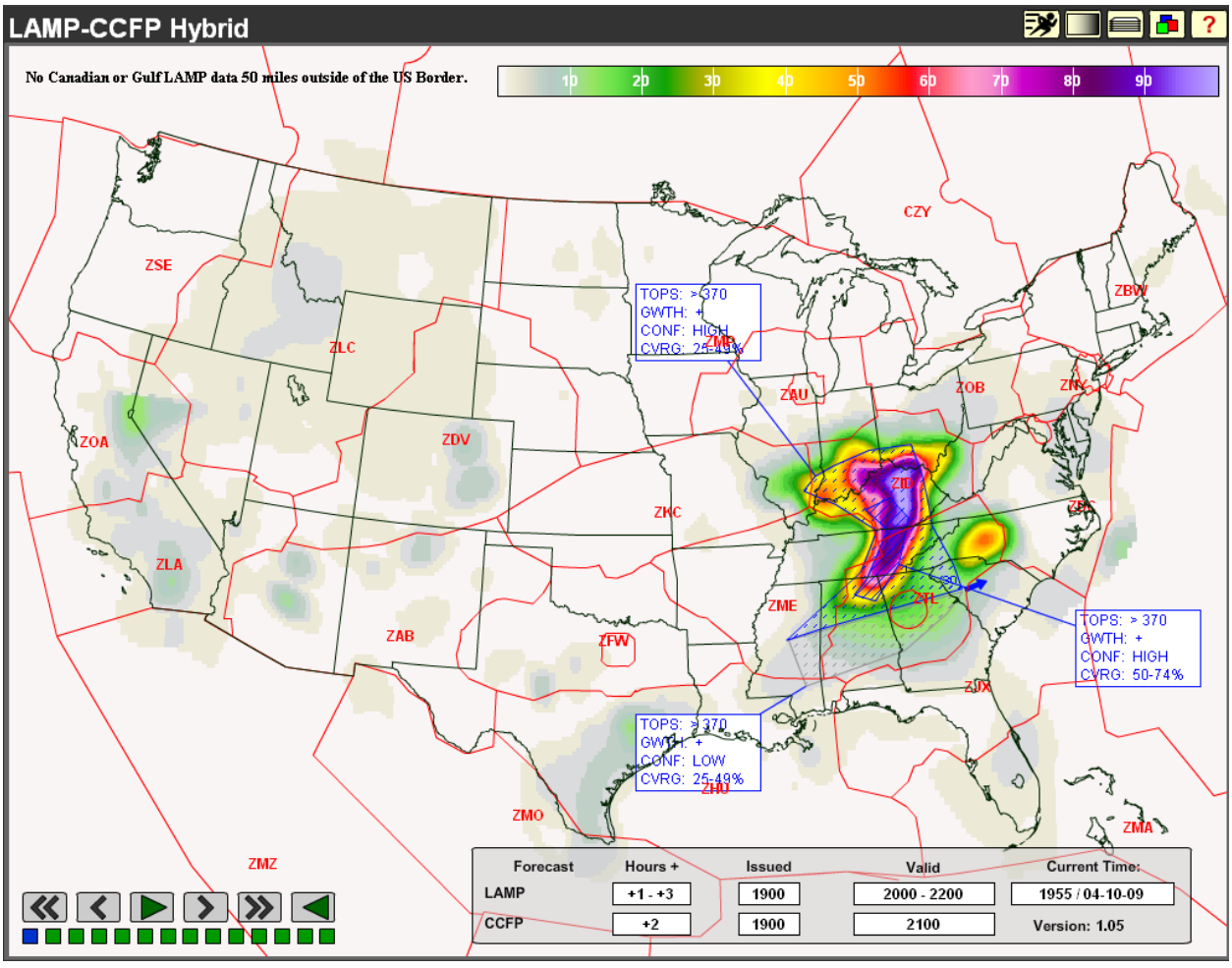

Figure 7. Experimental CCPF and LAMP thunderstorm probability "hybrid" product, where both LAMP and CCFP are based on the 1900 UTC cycle, 10 April 2009. The LAMP probability (%) is valid for the 2-h period of 2000 – 2200 UTC, whereas the CCFP is valid for the 2100 UTC "snapshot" time. Additional plotted information pertains to the CCFP product, which is described at http://weather.gov/infoservicechanges/CCFP_PDD_Enhancement.pdf.

6. ACKNOWLEGEMENTS

The LAMP thunderstorm program benefitted from the contributions of many NWS staff members. These include MDL members Judy Ghirardelli, who manages the overall LAMP program; Jerry Wiedenfeld (now with Weather Forecast Office Milwaukee, WI) and Scott Scallion, who were instrumental in LAMP's operational implementation; and Kathryn Gilbert and Phillip Shafer for providing the MOS thunderstorm probability equations and lightning data archive. Finally, David Kitzmiller, of the NWS Office of Hydrology, provided part of the radar reflectivity archive.

7. REFERENCES

Brier, G. W., 1950: Verification of forecasts in terms of probabilities. *Mon. Wea. Rev*., **78**, 1-3.

Charba, J. P., and F. Liang, 2005a: Automated two-hour thunderstorm guidance forecasts. Preprints, *Conference on Meteorological Applications of Lightning Data*. San Diego, CA, Amer. Meteor. Soc., CD-ROM **3.4**.

____, 2005b: Quality Control of gridded national radar reflectivity data. *21st Conf. on Weather Analysis and Forecasting*. Washington DC, Amer. Meteor. Soc., CD-ROM **6A.5**.

Charba, J. P., and F. Samplatsky, 2009a: Regionalization in fine grid quantitative precipitation forecasts. (Conditionally accepted for publication in *Mon. Wea. Rev*.).

____, 2009b: GFS-based MOS 6-h quantitative precipitation forecasts on a 4-km grid. (Manuscript in preparation).

Cummins, K. L., M. J. Murphy, E. A. Bardo, W. L. Hiscox, R. B. Pyle, and A. E. Pifer, 1998: A combined TOA/MDF technology upgrade of the U.S. national lightning detection network. *J. Geophys. Res.*, **103**, 9035-9044.

Ghirardelli, J., and B. Glahn, 2009: The Meteorological Development Laboratory's aviation weather prediction system. (Submitted to *Wea. Forecasting*).

Hughes, K. K., 2004: Probabilistic lightning forecast guidance for aviation. Preprints, *22th Conference on Severe Local Storms,* Hyannis, MA, Amer. Meteor. Soc., CD-ROM **2.6**.

Lowry, D. A., and H. R. Glahn, 1976: An operational model for forecasting probability of precipitation—PEATMOS PoP. *Mon. Wea. Rev.*, **109**, 221-232.

NWS, 2008: Terminal Aerodrome Forecasts. National Weather Service Instruction 10-813. National Oceanic and Atmospheric Administration, U.S. Department of Commerce, 60 pp.

Schaefer, T. J., 1990: The critical success index as an indicator of warning skill. *Wea. Forecasting*, **5**, 570-575.